Effectiveness of a super-pulsed CO_2 laser for removal of biofilm from three different types of implant surfaces: an in vitro study

Charles M. Cobb, DDS, MS, PhD, and Peter Vitruk, PhD, quantify implant surface decontamination parameters

Abstract

Background: As dental implants become a routine part of dental practice, so too will the prevalence of peri-implant diseases. Inherent to the treatment of peri-implant disease is the removal of microbial biofilms from the implant surface. Currently, there is no standardized protocol for application of any treatment modality directed at implant surface decontamination. In this in vitro study, we report on the effectiveness of a super-pulsed CO_2 laser (10.6 µm wavelength), delivering an average fluence of 6.3 to 113 J/cm^2, to remove biofilm from three different types of implant surface topographies.

Methods: Sixty-six implants representing three distinctly different surface topographies were used to prepare 132 specimens yielding 44 of each surface type. A 48-hour mixed species biofilm was established on the surface of each specimen. Controls consisted of untreated specimens while treated specimens were irradiated at eight different laser energy density (or fluence) levels ranging from 6.3 to 113 J/cm^2. Outcomes were measured by SEM examination and CFU counts of residual microbes following treatment at each fluence.

Results: Biofilms ranged in thickness from 5 to 15 µm. An average fluence of 19 J/cm^2 was sufficient to achieve 100% ablation of the biofilm on hydrophilic sandblasted and acid-etched surface specimens (SA). However, to achieve 100% ablation of biofilm on HA and highly crystalline, phosphate enriched titanium oxide (PTO) surfaced implants required an average fluence of 38 J/cm^2.

Conclusions: In this in vitro model, a 10.6 µm wavelength super-pulse CO_2 laser using parameters that produce an average fluence of 38 J/cm^2 will achieve 100% ablation of biofilms grown on implant specimens of varying topographies.

Charles M. Cobb, DDS, MS, PhD, graduated from the University of Missouri-Kansas City (UMKC), School of Dentistry in 1964. He received a Certificate of Specialty in Periodontics and a Master of Science degree in Microbiology, both from UMKC in 1966. Following two years of active duty with the U. S. Navy, Dr. Cobb returned to school at Georgetown University, graduating in 1971 with a PhD in Anatomy (emphasis in microanatomy). After graduation from Georgetown, he held teaching and research positions at Louisiana State University and the University of Alabama in Birmingham. Dr. Cobb devoted 15 years to full-time private practice in periodontics and 20 years to academics. He is a Diplomate of the American Board of Periodontology, has published over 200 peer-reviewed articles, and presented over 200 programs at regional, national, and international meetings. He recently concluded 1 year as the Interim Director of the Graduate Periodontics Program at UMKC. Lastly, Dr. Cobb retired from the U. S. Army Reserves with the rank of Colonel and is one of the few Reservists to be inducted into the Order of Military Medical Merit.

Peter Vitruk, PhD, MInstP, CPhys, is founder of LightScalpel, LLC, a member of the Science and Research Committee, Academy of Laser Dentistry, a member of the faculty of California Implant Institute and the faculty of Global Laser Oral Health, LLC.

Disclosure: Dr. Cobb reports no conflicts of interest related to this study. Dr. Vitruk is Founder of Luxarcare, LLC; Aesculight, LLC; and LightScalpel, LLC.

Introduction

As the placement of dental implants increases and becomes a routine part of dental practice so too will the prevalence rate of peri-implant diseases.[1] Some reports suggest the radiographic evidence of peri-implant bone loss may reach 30% to 35% while others report a lower rate, ranging from 10% to 20%.[2-7] The treatment of peri-implantitis, at some point, requires removal of all microbial biofilms from the exposed implant surface that, in turn, allows for optimal healing of host bone, osseous regeneration techniques, and overlying soft tissues.

Various methods of implant surface decontamination have been suggested, including use of tetracycline or sterile saline-soaked cotton pellets,[8-11] air-polishing with sodium bicarbonate,[12] diode,[13] Nd:YAG,[13] Er:YAG,[14] Er,Cr:YSGG,[15] and CO_2 lasers.[16] In addition, various adjunctive combinations with flap surgery and/or regenerative therapies have also been investigated.[8-10, 17,18] None of the prescribed methods of implant surface decontamination has been shown to be superior in the management of peri-implantitis. Part of the problem relates to the fact that there are no standardized protocols for any treatment modality directed at implant surface decontamination, including use of the CO_2 laser. Thus, the purpose of this in vitro project was to establish the minimum fluence at which complete microbial decontamination can be achieved using a super-pulsed CO_2 laser on each of three different, but common, implant surface topographies.

Materials and methods

Implants

Three implants types were selected that collectively represented a range of topography and surface roughness (Figure 1). The implants' surfaces were as follows:

1. hydroxyapatite (HA) plasma-sprayed (Steri-Oss® HA Coated Surface, Steri-Oss Inc.)
2. a highly crystalline, phosphate enriched titanium oxide surface produced by spark anodization (PTO) (NobelReplace™ Groovy, Nobel Biocare® USA)
3. hydrophilic sandblasted and acid-etched surface (SA) (Straumann® SLActive® Surface, Straumann USA, LLC)

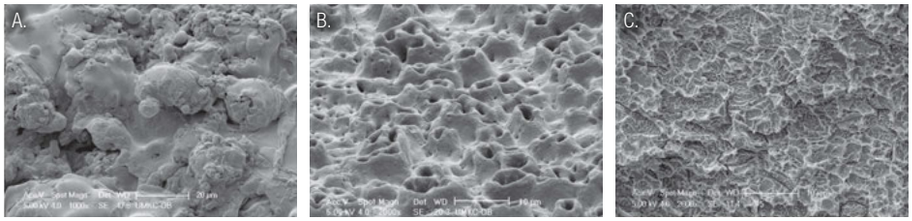

Figure 1: Untreated implant surfaces with no biofilm: (1A) HA plasma-spray coated. (1B) Untreated PTO. (1C) Untreated SA. Original magnification of x1,000; bar = 20 µm (1A); and x2,000; bar = 10 µm (1B, 1C)

From a total of 66 intact implants (22 of each surface type), two specimens measuring 1.0 mm (thickness) x 1.6 mm x 4.0 mm were cut from each 4.8 mm or 5.0 mm x 10 mm implant using a low-speed diamond saw (Buhler IsoMet® saw, Buhler). Specimens were cleaned of residual debris from the cutting process by sonication for 1 minute and rinsing twice, using sterile water. All implant specimens were sterilized by UV light exposure for 60 minutes[19] and then stored in sterile 48-well flat-bottomed cell culture dishes (Falcon® Cultureware, BD Biosciences) until inoculated and incubated with broth-containing bacteria.

A total of 44 specimens of each implant surface type were divided as follows:

- one untreated negative control (no biofilm for SEM), one untreated positive control (with biofilm for SEM), and one specimen from each of the eight laser treatment groups, all examined by SEM
- two untreated positive controls from each surface type to establish a baseline CFU count
- four treated specimens of each surface type from each of the eight different laser treatment groups used for CFU counts.

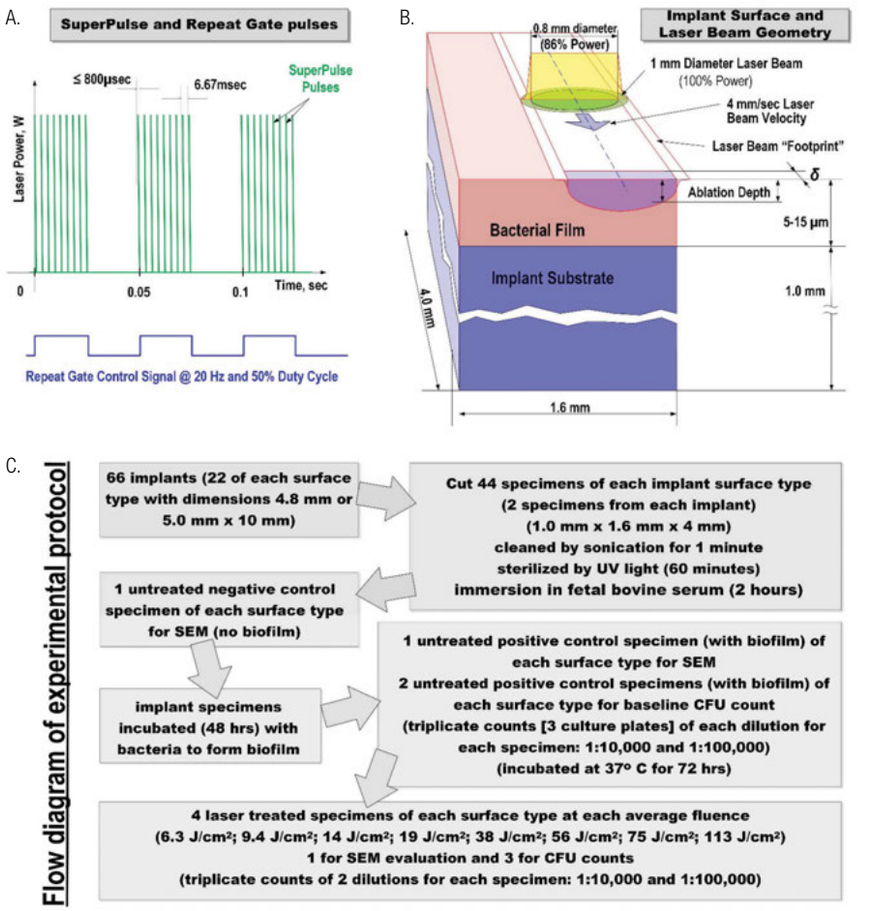

Figure 2: Drawings depicting (2A) repeat gating of SuperPulse modes with longer pulses (≥ 10 msec) at lower frequencies (≤ 30 Hz); (2B) movement of the laser beam over the biofilm adhering to the implant surface; and (2C) schematic of experimental protocol

Biofilm

Four supragingival plaque samples were obtained from each of five private practice periodontal patients exhibiting moderate and/or severe chronic periodontitis (i.e., ≥ 5 mm probing depth with bleeding on probing and radiographic evidence of interproximal bone loss). Samples were obtained during scaling and root planing appointments using a McCall 13S/14S curette. The technique and purpose of the plaque sampling was explained in detail to the volunteer patients.

All patients signed an informed consent according to the Helsinki Declaration.[20]

Plaque samples were pooled in 100 ml of broth media (Terrific Broth, Invitrogen®/ Life Technologies) and homogenized by vortex agitation for 1 minute. The pooled plaque sample was then incubated in a 150 ml roller bottle using a standard roller bottle apparatus under microaerophilic conditions at 37ºC for 48 hours. Following incubation, the 100 ml sample was agitated by vortex for 1 minute and then divided into four equal aliquots of 25 ml each. Fresh broth media was then added to each 25 ml aliquots, adjusting each to an absorption density of 1.0 (λ 630 nm) yielding four tubes of equal bacterial densities that were again agitated by vortex for 30 seconds. The resulting tubes of mixed bacteria were used as the stock sample for inoculation of the implant specimens. The inoculum contained approximately 106 microbes per ml.

Immediately prior to inoculating implant specimens with the bacteria-ladened broth, they were immersed for 2 hours in fetal bovine serum (Gibco® Fetal Bovine Serum, Life Technologies), which was diluted 1:1 in 25% sterile physiological saline. Preconditioning with fetal bovine serum served as a surrogate for GCF and salivary proteins that implants would normally acquire in situ. Using a 48-well sterile culture dish, three implant specimens of each surface type were placed in a single well and covered with 1.0 ml of stock solution (i.e., broth media) containing bacteria. The "inoculated" implants were then incubated on a shaker table (low setting for gentle agitation) at 37ºC in a microaerophilic environment for 48 hours. The resulting biofilm attached to the implant specimens ranged in thickness from 5 to 15 µm.

Laser

The laser used in this project was a Super-Pulsed CO_2 laser (10,600 nm) (Luxar NovaPulse LX-20SP CO_2 laser, LightScalpel, LLC). The laser handpiece LightScalpel PN LS9002-07 was fitted with a 0.8 mm spot size diameter ceramic delivery tip LightScalpel PN LS9005-01 (86% of beam energy contained within 0.8 mm diameter, 100% of energy contained within 1 mm diameter). The eight different fluence levels were determined by using the parameters listed in Table 1 (laser settings "A" through "H").

All laser settings were for SuperPulse mode (peak power > 50 W, pulse widths under 800 µsec, and pulse repetition rates of 150Hz. SuperPulse modes were further gated ("Repeat" gate settings, Table 1 and Figure 2A) with longer pulses (≥ 10 msec) at lower frequencies (≤ 30 Hz).

The pulse-width and pulse-rate settings of SuperPulse mode allow for thermal confinement of the laser energy deposited into 5-15 µm thick water-rich biofilm as will be discussed below.

A previous study[21] determined that when manually using a CO_2 laser to "paint" a flat surface, the typical rate of irradiation exposure is 4 mm/second. Thus, as all specimens measured 4 mm in length and 1.6 mm in width, each of two non-overlapping sweeps of the laser beam was of 1-second duration.

The laser handpiece was stabilized at a fixed 2 mm distance over the target surface by use of an adjustable-angle clamp attached to an L-shaped base support stand. Implant specimens were placed on a glass microscope slide that, in turn, was positioned on a variable speed motorized microscope stage, allowing passage of the specimen under the laser beam at the prescribed rate of 4 mm/second. This arrangement also allowed for minimal overlapping of exposed surfaces during the second pass required to cover the 1.6 mm width using the 0.8 mm diameter beam delivery tip (Figure 2B).

Following laser treatment of the implant specimen surface, the edges of the specimen were irradiated using a continuous beam and 6 Watts. This was to ensure that bacteria attached to the edges were ablated. Thus, only residual bacteria from the treated surface, if any, contributed to CFU counts.

Immediately following laser treatment, one specimen of each surface type from each treatment group was selected for SEM evaluation and immersed in fixative. The remaining three specimens were immersed in sterile broth media and processed for CFU counts. A summary schematic of the experimental protocol is presented in Figure 2C.

Colony-forming units

All laser treated implant specimens, including the eight untreated positive control specimens (with biofilm), were processed in a sterile laboratory hood in the following manner:

1. One implant specimen from each laser treatment group was randomly selected for SEM evaluation.
2. The remaining implant specimens were each immersed in 10 ml of fresh broth media and vigorously agitated by vortex for 2 minutes followed by 1 minute of sonication.
3. Serial dilutions were made from the supernatant (1:10,000 and 1:100,000).

Aliquots of 0.1 ml from each of the two dilutions were plated manually in triplicate using a spiral platter onto non-selective blood agar plates (Sigma-Aldrich) supplemented with hemin (5 mg/ml), menadione (1 mg/ml), and 5% sterile sheep blood. Plates were incubated under microaerophilic conditions at 37ºC for 72 hours.

Following incubation, the total number of CFU/ml was determined for each plate using an electronic colony counter system (Scienceware® Electronic Colony Counter System, Bel-Art Products). All counts were converted assuming a dilution of 1:100,000 and recorded as the average number of CFUs/ml. There was no attempt to subculture or identify recovered microbes other than by SEM morphotype.

Scanning Electron Microscopy

Specimens dedicated to SEM evaluation were immersed in ice-cold fixation consisting of 2.5% gluteraldehyde in 0.1 M cacodylate buffer at pH 7.4 for 2 hours. Following fixation, specimens were rinsed 3 times in 0.1 M cacodylate buffer (pH 7.4) for 5 minutes per rinse. Following the buffer rinse, specimens were dehydrated in a series of graded ethanol solutions (20% to 100%) at 5-minute intervals, followed by immersion in hexamethyldisilazane for 30 minutes. Each specimen was then affixed to an aluminum stub and stored in a desiccator overnight, followed by sputter-coating with approximately 20 nm of gold-palladium. Specimens were examined in a XL30 ESEM-FEG scanning electron microscope (FEI Corp., North America NanoPort) at various magnifications ranging from x80 up to x4,000. Magnifications of 2,000x and 4,000x were used to identify residual microbes by morphotype, i.e., coccus, short, medium, and long rods, fusiform, spirochete-like, and curved rods.

Statistical analysis

Regardless of implant surface topography, total decontamination of the implant surface is the clinical goal when treating peri-implant disease. Thus, the CFU data were log transformed to obtain only the main effect for each level of laser treatment. Descriptive statistics are presented for raw data and log-transformed CFUs. The measured outcome of laser treatment is the percentage reduction in CFU counts, assuming the baseline count of untreated implant specimens to represent 100%.

Results

The 48-hour biofilm that developed on the implant specimens ranged in thickness from 5 to 15 µm and was dominated by microbial morphotypes that were typically associated with a supragingival biofilms of natural teeth, i.e., cocci, short and medium length rods (Figure 3A). The morphologic character and thickness of the biofilm was consistent for all implant specimens regardless of the surface topography.

Table 1 summarizes the laser setting parameters and the results of the bacterial reduction, as well as the calculated depth of the laser ablation. It should be noted that 100% bacterial reduction was achieved at a fluence of 19 J/cm^2 (laser setting "D") per passage of the laser beam for the SA implant surface and for both the HA and PTO implant surfaces the bacterial reduction was 96.3% and 96.6%, respectively. At a fluence of 38 J/cm^2 (laser setting "E") or greater per pass, 100% of the biofilm was ablated and 100%

Table 1: Laser parameters used and percentage of bacterial reduction for each implant specimen surface type

Laser Setting #	Laser Display Power (W)	Repeat Gate Pulse Rate (Hz)	Repeat Gate Pulse Width (sec)	Average Fluence per Pass (J/cm^2)	SuperPulse Rate (Hz)	SuperPulse Fluence (J/cm^2)	Ablation Depth per SuperPulse pulse (µm)	Ablation Depth per Pass at 4mm/s (µm)	% Bacterial Reduction for HA implant	% Bacterial Reduction for PTC implant	% Bacterial Reduction for SA implant
A	2	10	0.01	6.3	150	2.29	0	0	53.6	59.0	71.4
B	3	10	0.01	9.4	150	3.44	2.1	4.8	62.4	71.4	69.3
C	3	15	0.01	14	150	3.44	2.1	7.2	83.3	87.0	92.4
D	3	20	0.01	19	150	3.44	2.1	9.6	96.3	96.6	100
E	4	30	0.01	38	150	4.59	7.4	52	100	100	100
F	4	30	0.015	56	150	4.59	7.4	78	100	100	100
G	4	30	0.02	75	150	4.59	7.4	104	100	100	100
H	6	30	0.02	113	150	6.88	18.1	254	100	100	100

bacterial reduction was measured regardless of the type of implant surface.

Use of per pass beam fluence of 6.3. 9.4, and 14 J/cm^2 (laser settings "A-C") achieved incomplete biofilm ablation and bacterial reduction, ranging from a low of 53.6% up to 92.4% with little variation between implant surface types (Table 1). SEM examination of specimens treated with a fluence of ≤ 14 J/cm^2 revealed the presence of residual microbes (incomplete biofilm ablation) within surface depressions (Figures 3B and 3C). At a beam fluence of 38 J/cm^2 (laser setting "E"), it was noted that the HA surface exhibited evidence of melting (Figure 3D), whereas the PTO and SA surfaces showed no surface alterations at any of the higher fluence exposures, i.e., 38, 56, 75, and 113 J/cm^2.

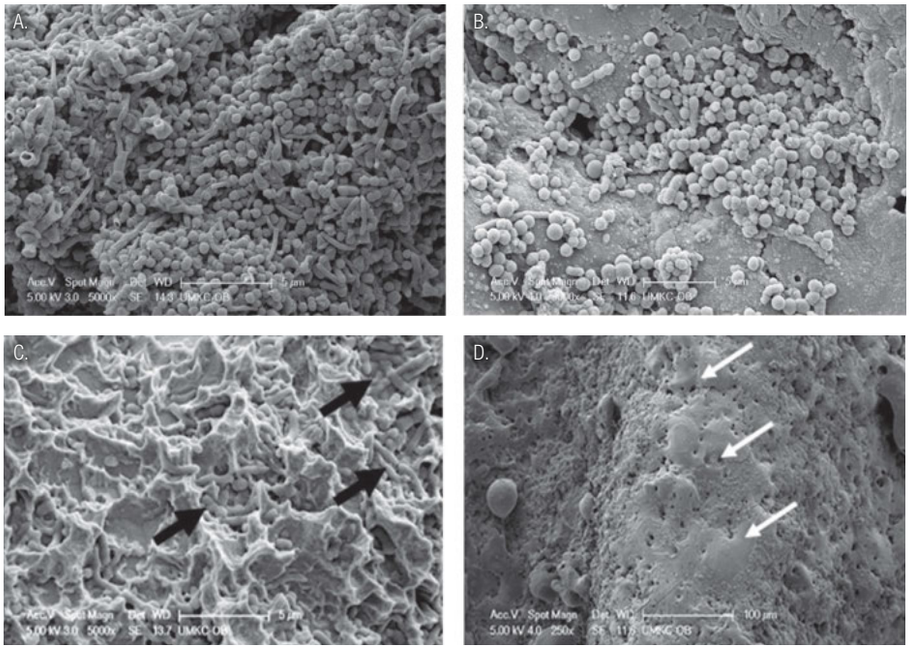

Figures 3A-3D: High magnification SEM photographs. 3A. 72-hour in vitro biofilm growth on SA implant surface (Average thickness of biofilm for all implant specimens was ≈ 10 µm with a range of ≈ 5-15 µm. Original magnification x5,000; bar = 5 µm). 3B. HA implant surface showing residual microbes following laser treatment using a fluence of 14 J/cm2 per pass of the laser beam. Original magnification of 4,000x; bar = 5 µm. 3C. PTO implant surface following laser treatment using a fluence of 14 J/cm2 per pass of the laser beam. Arrows indicate residual cocci and short rod microbes lying within surface depressions. Original magnification of 5,000x; bar = 5 µm. 3D. HA plasma-sprayed coated implant surface exhibiting evidence of surface melting (arrows) following treatment using a fluence of 38 J/cm2 per pass of the laser beam. Original magnification of 250x; bar = 100 µm

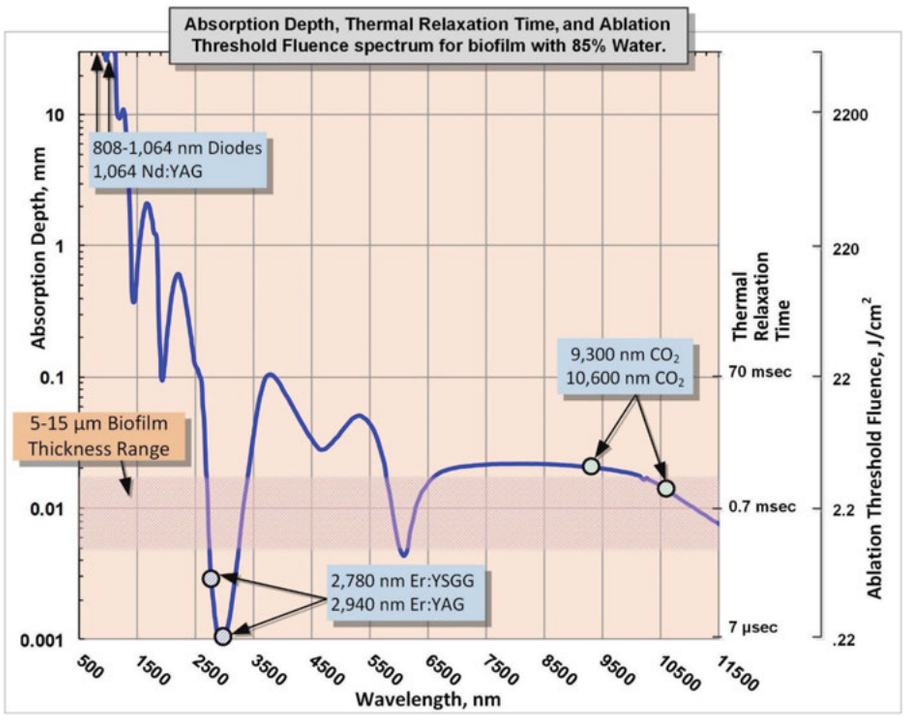

Figure 4: Absorption depth, Thermal Relaxation Time, and ablation threshold fluence spectrum for biofilm with assumed 85% water content

Discussion

Efficient bacterial reduction can be achieved by ablating the bacterial biofilm off the implant surface without heating nor damaging the implant if:

1. Laser energy is efficiently deposited into the biofilm.
2. Laser-generated heat inside the biofilm is confined to the biofilm and is not thermally conducted away into the body of the implant (which acts as a highly efficient heat sink).
3. Laser-generated heat inside the biofilm is sufficient for vaporizing the biofilm.

The first condition (efficient laser energy deposition into the biofilm) is met when laser absorption depth is comparable to the biofilm's thickness. Figure 4 presents absorption depth and thermal relaxation time spectra[22] for a biofilm assumed to have a water content of 85%.[23] The absorption depth of a 10.6 µm wavelength CO_2 laser wavelength is about 14 µm, which is well within the range of the biofilm thickness observed in this study, i.e., range of 5 to 15 µm.

The second condition of thermal confinement of laser energy within the irradiated biofilm is met when the laser pulse duration is shorter than Thermal Relaxation Time (**TRT**), also presented in Figure 4. **TRT** defines the rate of how fast the irradiated tissue diffuses the heat away as defined through the thermal diffusion time: $\mathbf{TRT = A^2/K,}$[24,25] where A is optical absorption depth discussed above. The physics behind thermal diffusivity process is similar to diffusion and Brownian motion first described by Einstein in 1905.[26] Coefficient $\boldsymbol{K}$ is the tissue's thermal diffusivity; $\boldsymbol{K} = \lambda / (\varrho\ C) \approx 0.155$ (+/-0.007) mm^2/sec (derived from heat conductivity $\lambda \approx 6.2$-6.8 mW/cm ºC; specific heat capacity $\boldsymbol{C} \approx 4.2$ J/g ºC, and density $\varrho \approx 1$ g/cm^3 for liquid water for temperatures in 37ºC-100ºC range).[27] For 10 µm thick 80%-90% water-rich biofilm at 10,600 nm wavelength, the **TRT** is approximately 700 µsec. Therefore, a SuperPulsed CO_2 laser with pulses under 800 µsec are highly efficient at confining the heat generated by the laser pulse within the biofilm thickness during the laser pulse.

The third condition of efficient biofilm vaporization (or ablation) is met when laser

fluence during the SuperPulse pulse exceeds laser ablation threshold E_{th}[25,28] presented in Figure 4. The more efficiently the laser energy is absorbed (Erbium and CO_2 lasers), the lower is the ablation threshold. The less efficient the laser energy is absorbed (diode and Nd:YAG lasers), the higher is the ablation threshold. The ablation threshold at the 10.6 µm CO_2 laser's wavelength for a biofilm with an assumed 85% water content equals approximately 3 J/cm^2. Laser settings "B-H" from Table 1 with fluence over 3 J/cm^2 fit the ablative requirements.

During each SuperPulse pulse, the ablation depth δ is given by the formula $\delta = A\,(E - E_{th}) / E_{th}$ for the steady state ablation conditions,[25] where A is the absorption depth and E_{th} is the ablation threshold fluence, and E is the fluence during the SuperPulse pulse. Ablative laser settings "B-D" in Table 1 (with fluence over 3 J/cm^2) allow for an ablation depth of approximately 2-18 µm per pulse; multiple pulses stacked on top of each other allow for deeper ablation depths (proportional to number of pulses).

Bacterial reduction depends on how much of the bacterial biofilm is ablated as illustrated in Figure 5. Bacterial reduction of 100% can be achieved only through complete laser ablation of the biofilm; the sub-ablative laser setting "A" with 2.29 J/cm^2 is seen as the least efficient.

As also observed in this study, plasma-sprayed hydroxyapatite HA implant surface is susceptible to melting and heat-induced cracking at an average fluence greater than 19 J/cm^2 and certainly at the 38 J/cm^2 as noted in this study. This can be explained through high absorption of the 10,600 nm light by the hydroxyapatite[29] exposed after the bacterial biofilm was ablated. In contrast, the PTO and SA surfaces did not exhibit adverse surface interactions even at higher fluences up to 113 J/cm^2, which can be explained by high reflectivity of titanium (> 90%) at 10,600 nm.[30]

Conclusion

An average fluence of 19 J/cm^2 delivered by a SuperPulse 10.6 µm wavelength CO_2 laser is sufficient to achieve a 100% ablation of an in vitro biofilm of approximately 10 µm thickness grown on implant specimens with a moderately rough surface topography. A similar reduction on HA or highly crystalline, phosphate enriched titanium oxide surfaces required an average fluence of 38 J/cm^2. The HA surface implant specimens also exhibited surface melting and heat crazing at an average fluence of 38 J/cm^2. The SuperPulse 10.6 µm wavelength CO_2 laser may provide a predictable method of surface decontamination in the treatment of peri-implantitis. IP

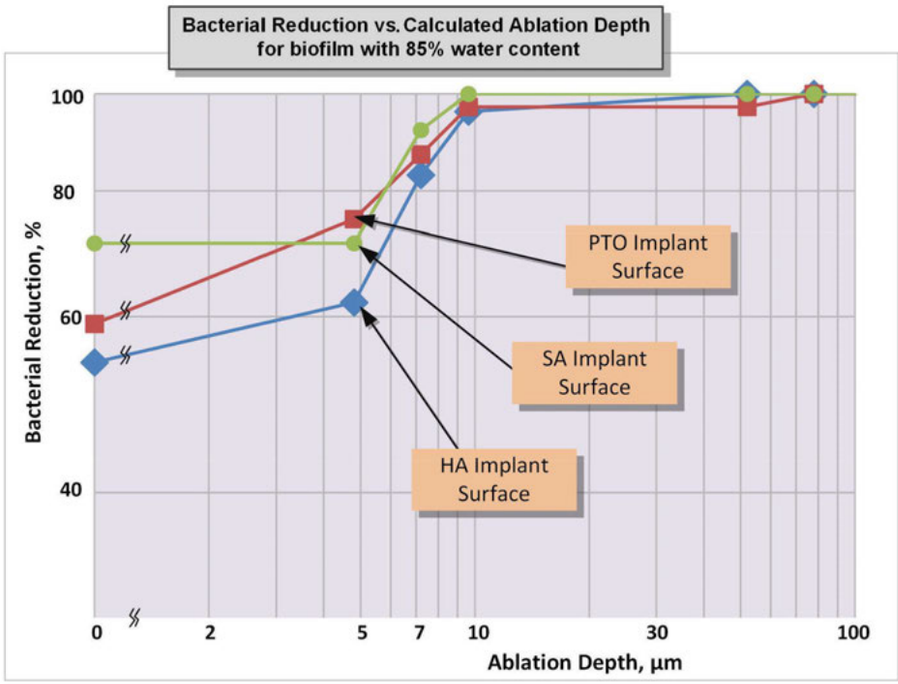

Figure 5: Bacterial reduction vs. calculated ablation depth for 10 µm thick biofilm with an assumed 85% water content

REFERENCES

1. Da Silva JD, Kazimiroff J, Papas A, Curro FA, Thompson VP, Vena DA, Wu H, Collie D, Craig RG. Outcomes of implants and restorations placed in general dental practices: A retrospective study by the Practitioners Engaged in Applied Research and Learning (PEARL) Network. *J Am Dent Assoc.* 2014;145(7):704-713.
2. Roccuzzo M, Bonino F, Aglietta M, Dalmasso P. Ten-year results of a three arms prospective cohort study on implants in periodontally compromised patients. Part 2: Clinical result. *Clin Oral Implants Res.* 2012;23(4):389-395.
3. Renvert S, Lindahl C, Rutger-Persson G. The incidence of peri-implantitis for two different implant systems over a period of thirteen years. *J Clin Periodontol.* 2012;39(12):1191-1197.
4. Fardal O, Grytten J. A comparison of teeth and implants during maintenance therapy in terms of the number of disease-free years and costs – an in vivo internal control study. *J Clin Periodontol.* 2013;40(6):645-651.
5. Gruica B, Wang HY, Lang NP, Buser D. Impact of IL-1 genotype and smoking status on the prognosis of osseointegrated implants. *Clin Oral Implants Res.* 2004;15(4):393-400.
6. Koldsland OC, Scheie AA, Aass AM. Prevalence of peri-implantitis related to severity of the disease with different degrees of bone loss. *J Periodontol.* 2010;81(2):231-238.
7. Mombelli A, Müller N, Cionca N. Epidemiology of peri-implantitis. *Clin Oral Implants Res.* 2012;23(Suppl 6):67-76.
8. Schmidt EC, Papadimitriou DEV, Caton JG. Surgical management of peri-implantitis: A clinical case report. *Clin Adv Periodontics.* 2014;4(1):31-37.
9. Aljateeli M, Fu JH, Wang HL. Managing peri-implant bone loss: current understanding. *Clin Implant Dent Related Res.* 2012;14(Suppl 1):e109-e118.
10. Froum SJ, Froum SH. Rosen PS. Successful management of peri-implantitis with a regenerative approach: A consecutive series of 51 treated implants with 3- to 7.5-year follow-up. *Int J Periodontics Restorative Dent.* 2012;32(1):11-20.
11. Heitz-Mayfield LJ, Salvi GE, Mombelli A, Faddy M, Lang NP. Anti-infective surgical therapy of peri-implantitis. A 12-month prospective clinical study. *Clin Oral Implants Res.* 2012;23(2):205-210.
12. Vouros JD, Papadopoulos C, Menexes G, Konstantinidis A. Laser and air-abrasive therapies in the nonsurgical treatment of peri-implantitis: A systemic review. J *Implant Adv Clin Dent* 2014;6:21-36.
13. Goncalves F, Zanetti AL, Zanetti RV, Martelli FS, Avila-Campos MJ, Tomazinho LF, Granjeiro JM. Effectiveness of 980-mm diode and 1064-nm extra-long-pulse neodymium-doped yttrium aluminum garnet lasers in implant disinfection. *Photomed Laser Surg.* 2010; 28(2):273-280.
14. Yamamoto A, Tanabe T. Treatment of peri-implantitis around TiUnite-surface implants using Er:YAG laser microexplosions. *Int J Periodontics Restorative Dent.* 2013;33(1):21-30.
15. Schwarz, F, Nuesry E. Bieling K. Herten M., Becker J. Influence of an erbium, chromium- doped yttrium, scandium, gallium, and garnet (Er,Cr:YSGG) laser on the reestablishment of the biocompatibility of contaminated titanium implant surfaces. *J Periodontol.* 2006;77(11): 1820-1827.
16. Romanos GE, Nentwig GH . Regenerative therapy of deep peri-implant infrabony defects after CO2 laser implant surface decontamination. *Int J Periodontics Restorative Dent.* 2008;28(3):245-255.
17. Schwarz F, Sahm N, Iglhaut G, Becker J. Impact of the method of surface debridement and decontamination on the clinical outcome following combined surgical therapy of peri- implantitis: a randomized controlled clinical study. *J Clin Periodontol.* 2011;38(3):276-284.
18. Schwarz F, John G, Mainusch S, Sahm N, Becker J. Combined surgical therapy of peri-implantitis evaluating two methods of surface debridement and decontamination. A two-year clinical follow up report. *J Clin Periodontol.* 2012; 39(8):789-797.
19. Sharma A. An ultraviolet-sterilization protocol for microtitre plates. *J Exp Microbiol Immunol.* 2012;16:144-147.
20. World Medical Association Declaration of Helsinki: ethical principles for medical research involving human subjects. *JAMA.* 2013(20);310:2191-2194.
21. Spencer P, Cobb CM, McCollum MH, Wieliczka DM. The effects of CO2 laser and Nd:YAG with and without water/air surface cooling on tooth root structure: Correlation between FTIR spectroscopy and histology. *J Periodontol Res.* 1996;31(7):453-462.
22. Jacques SL. Optical properties of biological tissues: a review. *Phys Med Biol.* 2013;58(11):R37-61.
23. Zhang XQ, Bishop PL, Kupferle MJ. Measurement of polysaccharides and proteins in biofilm extracellular polymers. *Water Sci Technol.* 1998;37:345-348.
24. Svaasand LO. Lasers for biomedical applications. In: Driggers RG, ed. *Encyclopedia of Optical Engineering.* New York, NY: Marcel Dekker; 2003:1035-1041.
25. Vogel A, Venugopalan V. Mechanisms of pulsed laser ablation of biological tissues. *Chem Rev.* 2003;103(2):577-644.
26. Einstein A. Über die von der molekularkinetischen Theorie der Wärme geforderte Bewegung von in ruhenden Flüssigkeiten suspendierten Teilchen. *Annalen der Physik.* 1905;322(8):549-60.
27. Weast RC, ed. *CRC Handbook of Chemistry and Physics.* 61st ed. Boca Raton, FL: CRC Press; 1980-1981.
28. Vitruk P. Oral soft tissue laser ablative and coagulative efficiencies spectra. *Implant Practice US.* 2014;7(6):22-27.
29. Duplain G, Boulay R, Bélanger PA. Complex index of refraction of dental enamel at CO2 laser wavelengths. *Appl Opt.* 1987; 26(20):4447-4451.
30. Wolfe WL, Zissis GJ. *The Infrared Handbook.* Washington DC: Office of Naval Research, NAVY, 1985:7-81.